Theoretical Mathematics & Applications, vol.6, no.4, 2016, 53-69
ISSN: 1792-9687 (print), 1792-9709 (online)
Scienpress Ltd, 2016

A Numerical Method for Prediction of Masses of Real Particles, e.g. Neutrinos

Ulrich E. Bruchholz[1] **and Horst Eckardt**[2]

Abstract

It is shown how particle quantities like masses of supposed neutrinos can be computed on base of a classical theory. The numerical method is based on discretization of differential equations which is being used successfully in some parts of theoretical physics but is underestimated wrongly for application to particles. The method is explained by an ordinary differential equation first. Then it is demonstrated how this simple method proves successful for non-linear field equations with chaotic behaviour. Integration constants of the field equations enter the method in form of parameters. Using certain discrete values of the integration constants, a chaos-like behaviour comparable with MANDELBROT sets is obtained. The known EINSTEIN-MAXWELL equations are investigated, where discrete particle quantities are obtained from a continuous theory which is possible only by this method. Known particle values are confirmed, and unknown values can be predicted. In this paper, supposed neutrino masses are presented.

Mathematics Subject Classification: 35-04; 35Q61; 35Q75; 35Q90; 65-04;

[1] Independent. Email: Ulrich.Bruchholz@t-online.de
[2] Independent. Email: mail@horst-eckardt.de

Article Info: *Received* : January 17, 2016. *Revised* : March 8, 2016.
Published online : October 30, 2016.

65E05; 65M06; 65M22; 65M38; 65N22; 65N25; 65Q10; 65Y99; 65Z05; 83-04; 83C22; 83C99
Keywords: Numerical methods; Non-linear systems; Chaos; Geometric theory of fields; Particle characteristics

1 Introduction

Although the discretization of differential equations was introduced more than fourty years ago, the power of this method has not fully been recognized in all fields of science. In particular, difficult problems of theoretical physics, for example in the field of general relativity, have traditionally been tried to solve by rough analytical approximations instead of using numerical methods. In the last two decades, however, collisions of black holes have been computed numerically [1] for example, and other detailed problems of relativity. This gives us confidence that numerical methods are applicable in all fields of theoretical physics and can even reveal new insights which were not accessible by simple analytical models.

An example of successful application of numerics is the field of chaos research. Common literature on chaos is for example [2, 3]. The well known MANDELBROT set is not possible to be inspected without usage of numerical calculations on a computer. The convergence behaviour per starting point in a plane can be graphed nicely. We proceed similarly in this paper, basing the calculation on solutions of differential equations rather than simple iteration formulae. The basic calculation scheme is presented in section 2.

As for the physical background, the standard theory being used for describing structure of matter on nuclear and subatomic level is based on considerations of symmetry and was successful in constructing a classification scheme of sub-atomic particles. This theory, although considered as being "the best we have", has a number of shortcomings. It cannot be unified with general relativity and there is no way to compute masses of elementary particles by a method based on first-principles. Instead, masses of sub-atomic and elementary particles (as well as other properties) have to be introduced as adaptable parameters. Although there were attempts in the past to overcome this problem, these approaches have not been considered in mainstream physics up to

date. They are simply precluded in context with particles. One of these approaches is the unification of electromagnetism with general relativity by the Einstein-Maxwell theory which the work of this paper is based on. The resulting geometry from Einstein's equation using the energy-momentum tensor of electrodynamics was found by Rainich [5, 6] already in 1924. The related equations are explained in section 3.1. In section 3.2, details of the computational method for obtaining quantities of elementary particles are discussed. The results for neutrinos are presented, and compared with results for atomic nuclei and the electron in section 3.3. While the masses of neutrinos could not be determined exactly up to now, we present a prediction based on our calculations which lies within the error limits safely known by experiment.

The method works well on the basis of inherent information in the electrovacuum around the particle. It utilizes the inherent chaos of the Einstein-Maxwell equations. The numerical method in general is explained in the next section.

2 Explanation of the Numerical Method

In direct numerical solutions of differential equations the differential quotient is replaced by a quotient of finite differences. This leads to recursion rules on the calculational grid. In the following we will derive a scheme of differences which is suitable for the type of problems we will solve in section 3.2. We consider a differential equation of the form

$$f''(x, c_\nu) + F(x, f'(x), c_\nu) = 0 \tag{1}$$

where F is a function of the derivative of the function $f(x)$ to be found. F and f depend on a set of constants c_ν. The function values at discrete points x_n shall be denoted by f_n. With difference quotients

$$\frac{\partial f}{\partial x}\Big|_{x_n} = \frac{f_{n+1} - f_{n-1}}{2\ \Delta x} \tag{2}$$

and for the second derivative

$$\frac{\partial^2 f}{\partial x^2}\Big|_{x_n} = \frac{f_{n+2} - 2f_n + f_{n-2}}{(2\ \Delta x)^2} \tag{3}$$

we obtain a recursion formula for the discrete function value of f at x_{n+2}:

$$f_{n+2} = 2f_n - f_{n-2} - (2\ \Delta x)^2 F_n(c_\nu) \tag{4}$$

or, rewritten,

$$f(x + 2\ \Delta x) = 2f(x) - f(x - 2\ \Delta x) - (2\ \Delta x)^2 F(x - \Delta x, x, x + \Delta x, c_\nu)\ . \tag{5}$$

We have chosen a difference of two grid points for the second derivative in order to obtain a simple recursion formula. The parameters c_ν denote the integration constants of the differential equations and are part of the initial conditions. The latter are obtained from appropriate approximations of f in the initial range of x. For real-valued x and c_ν this iteration formula is able to behave in a chaotic manner, in dependence of the parameters c_ν. These results can be generalized for systems of partial differential equations with many variables. In definition regions where the functions have diverging solutions, we obtain a map of the "degree of divergence" which can be graphed in a plane if we have two parameters c_1 and c_2 for example.

We shall see from the Einstein-Maxwell equations that different values of the integration constants (as parameters) lead to a varying divergence behaviour. While f immediately diverges in most cases, there are discrete values of the parameters c_ν where f diverges at a relatively sharply defined x value which stands for the radius here. (Further details are given in section 3.2.) These special values of the parameters represent a special set leading to a kind of "semi-stable" solutions of f. – In practice, this behaviour will be smeared over due to rounding errors. (Otherwise, we would not find the relevant discrete values.)

3 Demonstration of the Numerical Method with Einstein-Maxwell Equations

3.1 The equations

The theory is based on the relativistic tensor equations [8] of Riemannian geometry:

$$R_{ik} = \kappa\ (\frac{1}{4}\ g_{ik} F_{ab} F^{ab} - F_{ia} F_k{}^a) \quad , \tag{6}$$

$$F_{ij,k} + F_{jk,i} + F_{ki,j} = 0 \quad , \tag{7}$$

$$F^{ia}{}_{;a} = 0 \quad , \tag{8}$$

in which g_{ik} are the components of metrics, R_{ik} those of the RICCI tensor and F_{ik} those of the electromagnetic field tensor. κ is EINSTEIN's gravitation constant. The partial derivative is denoted by a comma, the covariant derivative by a semicolon. If we express the field tensor by a vector potential $\mathbf{A}$ with

$$F_{ik} = A_{i,k} - A_{k,i} \quad , \tag{9}$$

equation (7) is identically fulfilled. Thus, we can base our calculations on quantities having the character of potentials that are metrics and the electromagnetic vector potential.

These equations are known as EINSTEIN-MAXWELL equations. The energy-momentum tensor of electrodynamics is equated to the energy-momentum tensor of EINSTEIN's theory [4]. In detail, the *homogeneous* MAXWELL equations are used. Only these fulfill force equilibrium and conservation of energy and momentum (mathematically expressed by the BIANCHI identities). These equations describe the electro-vacuum around a particle and involve geometry described by the EINSTEIN part (equation (6)) of the equations. The involved geometry was found by RAINICH already in the year 1924 [5, 6].

We shall use these equations as an example in what follows, not considering the physical significance they may or may not have. This significance will become visible by the achieved results.

The sources of related inhomogeneous equations [4] are the right-hand side of

$$R_{ik} - \frac{1}{2}\, g_{ik} R = -\kappa T_{ik} \tag{10}$$

with

$$T^{ik} = \sigma \frac{\mathsf{d}x^i}{\mathsf{d}s} \frac{\mathsf{d}x^k}{\mathsf{d}s} \tag{11}$$

(σ = mass density) for distributed masses and momenta, and

$$F^{ia}{}_{;a} = S^i \tag{12}$$

for distributed charges and currents.

Equation (10) was introduced by EINSTEIN and GROSSMANN, and equations

(7), (12) actually are the covariant MAXWELL equations. The sources are replaced by integration constants [7]. Mass, spin, electric charge, and magnetic moment are the first integration constants. It is demonstrated in [7] how to determine the integration constants of geometric equations from integrals of sources.

These equations yield only 10 independent equations for 14 components g_{ik}, A_i. It will be demonstrated that the omnipresent quantization has nothing to do with this indeterminacy. The quantization is the consequence from the chaotic behaviour of these geometric equations, even also if we override the indeterminacy of the above variables with additional conditions. – We will consider only the diagonal elements of g_{ik} plus two off-diagonal elements for practical calculations, which reduces the number of equations.

3.2 Numerical calculations

Analytic solutions of equations (6, 8, 9) commonly lead to singularities. There are two types of singularities. The first type is a singularity inferred by assuming point masses and charges in order to simplify the equations so that analytical solutions are feasible. This is often considered as a deficit when comparing a calculation with the situation in reality. However, in our calculations, these formal singularities are placed into the inner of the particle (according to observer's coordinates) which is not subject of calculation. With spherical coordinates, the formal singularity is at the centre. This is the first type of singularity.

The basic idea of calculation is as follows. The equations (6, 8, 9) are evaluated on a radial grid from outer to inner and so one approaches the unknown inner region successively. At a certain radius, the calculation starts to diverge because the central singularity becomes predominant. It is important to notice that this radius of divergence is clearly separated from the central singularity so a second type of singularity, a "numerical singularity" here appears. This is the "chaos behaviour" we want to investigate.

The numerical simulations according to the EINSTEIN-MAXWELL equations show that the numerical singularity is not a problem, for the following reason: Numerical simulations using iterative, non-integrating methods lead always to a boundary at the conjectural particle radius. As a result, the second

singularity is always within a geometric limit, i.e. a geometric distance from the centre. The region within this geometric limit *according to observer's coordinates* is not accessible to further investigation but this is even not required. The geometric limit is the mathematical reason for the existence of discrete "semi-stable" (explained in section 2) solutions. This has to do with chaos, see [7] and previous sections. These discrete solutions involve discrete values of the integration constants, which are also called eigenvalues. We shall see that the electro-vacuum is able to produce such eigenvalues, and that the eigenvalues perform a set identical with the entirety of the particle characteristics.

In order to gain eigenvalues, one has to do lots of tests, because the particle quantities are integration constants and have to be inserted into the initial conditions (for more details see [7]), which are defined for the electro-vacuum around the particle.

As already mentioned, the basis for computations are equations (6, 8, 9). For the sake of simplicity, we restrict equations (6, 8, 9) to time independence and rotational symmetry. That results, with spherical coordinates

$$x^1 = r \ , \ x^2 = \vartheta \ , \ x^3 = \varphi \ , \ x^4 = \mathsf{j}ct \ ,$$

in 6 independent equations for 8 components with character of a potential, $A_3,\ A_4,\ g_{11},\ g_{12},\ g_{22},\ g_{33},\ g_{34},\ g_{44}$, the other vanish. In order to override the indeterminacy by the two missing equations, we define

$$g_{12} = 0 \qquad \text{(and, consequently, } g^{12} = 0) \tag{13}$$

and

$$g = \det |g_{ik}| = r^4 \sin^2 \vartheta \quad . \tag{14}$$

These conditions are arbitrary, in which the second is taken from the free-field Minkowski metric. In combination, they are leading to reasonable results.

The integration constants from equations (6, 8, 9) result from a series expansion. The first coefficients of expansion are the input for the simulations and are inserted into the initial conditions [7]. The output is the number of grid points along the radius until divergence occurs, which is a measure for the stability of the solution.

The first coefficients (integration constants) are

$$c_1 = -\ \frac{\kappa\ m}{4\pi} \Longrightarrow \frac{\kappa\ m}{4\pi} \tag{15}$$

(mass),

$$c_2 = \mathsf{j}\ \frac{\kappa\ s}{4\pi c} \Longrightarrow \frac{\kappa\ s}{4\pi c} \tag{16}$$

(spin),

$$c_3 = -\mathsf{j}\ \frac{{\mu_\circ}^{\frac{1}{2}}\ Q}{4\pi} \Longrightarrow \frac{\kappa^{\frac{1}{2}}\ {\mu_\circ}^{\frac{1}{2}}\ Q}{4\pi} \tag{17}$$

(charge), and

$$c_4 = -\ \frac{{\varepsilon_\circ}^{\frac{1}{2}}\ M}{4\pi} \Longrightarrow \frac{\kappa^{\frac{1}{2}}\ {\varepsilon_\circ}^{\frac{1}{2}}\ M}{4\pi} \tag{18}$$

(magnetic moment).

As explained, these follow from a comparison of series expansion from the Einstein-Maxwell equations (homogeneous Maxwell equations) with the solutions of equivalent inhomogeneous equations, see [7]. The dimensionless terms after the arrow are taken for computation, and have positive values. The imaginary unit has been eliminated. The unit radius ($r = 1$) corresponds to 10^{-15}m. By this, the initial conditions become, using $T = \frac{\pi}{2} - \vartheta$,

$$g_{11} = 1 + \frac{c_1}{r} - \frac{1}{2}(\frac{c_3}{r})^2 + \frac{(\frac{c_4}{r^2})^2(1+\cos^2 T)}{10}, \tag{19}$$

$$g_{22} = r^2\{1 + (\frac{c_4}{r^2})^2(\frac{1}{3}\cos^2 T - \frac{3}{10})\}\ , \tag{20}$$

$$g_{33} = r^2\cos^2 T\{1 + (\frac{c_4}{r^2})^2(\frac{\cos^2 T}{15} - \frac{3}{10})\}\ , \tag{21}$$

$$g_{44} = 1 - \frac{c_1}{r} + \frac{1}{2}\{(\frac{c_3}{r})^2 + (\frac{c_4}{r^2})^2\sin^2 T\}\ , \tag{22}$$

$$g_{34} = r\cos^2 T\ (\frac{c_2}{r^2} - \frac{1}{2}\frac{c_3 c_4}{r^3})\ , \tag{23}$$

$$A_3 = r\cos^2 T\ \frac{c_4}{r^2}\ , \tag{24}$$

$$A_4 = \frac{c_3}{r}\ . \tag{25}$$

The physically relevant parts of the metrical components are called physical metric components. These are the complement to unity in equations (19-22). Denoting the complements by $g_{(11)}$ etc. the above equations read

$$g_{11} = 1 + g_{(11)}\ , \tag{26}$$

$$g_{22} = r^2\,(1 + g_{(22)})\ , \tag{27}$$

$$g_{33} = r^2\sin^2\vartheta\,(1 + g_{(33)})\ , \tag{28}$$

$$g_{44} = 1 + g_{(44)}\ . \tag{29}$$

The physical metric components have a magnitude of ca 10^{-40}. Since several components contain unities, the physical components would have no effect due to lack of numerical precision during computation. Therefore, the actual computation is done with quantities performed from these physical components, with the consequence that the unity summands in the equations are eliminated.

We have to insert the values of the integration constants into the modified initial conditions (with physical components), see program in the data package (available at the author's website[3]). The conversion of physical into normalized (dimensionless) values and vice versa is described in detail in [7, 10]. Table 1 shows some values with radius unit of 10^{-15}m. These examples allow for convenient conversion.

Table 1: Physical and normalized values for conversion

	physical value	norm. value
proton mass	1.672×10^{-24}g	2.48×10^{-39}
electr. mass	0.911×10^{-27}g	1.35×10^{-42}
$\hbar$	1.054×10^{-27}cm^{2}g/s	5.20×10^{-40}
elem. charge	1.602×10^{-19}As	1.95×10^{-21}
μ_B	1.165×10^{-27}Vs cm	3.70×10^{-19}

Higher moments are missing in the equations because of lack of knowledge, their influence is estimated to be rather small. In the results section we will insert known values and values deviating from them, and compare the results.

The algorithm for evaluating the equations requires numerical differentiation. We do this by separating the quantity with highest radius index at the left-hand side as described in section 2. All previously evaluated quantities are at the right-hand side. These quantities come from equations (6) and (8) using (9). For example when we calculate spherical shells from outside to inside, the new quantity is $f_{m+2,n}$. In the following difference equations f stands for *any*

[3]http://www.bruchholz-acoustics.de/physics/neutrino_data.tar.gz

potential-like quantity:

$$\frac{\partial f}{\partial r}\Big|_{r_m,T_n} = \frac{f_{m-1,n} - f_{m+1,n}}{2\ \Delta r}\ , \tag{30}$$

$$\frac{\partial^2 f}{\partial r^2}\Big|_{r_m,T_n} = \frac{f_{m+2,n} - 2f_{m,n} + f_{m-2,n}}{(2\ \Delta r)^2}\ , \tag{31}$$

$$\frac{\partial f}{\partial T}\Big|_{r_m,T_n} = \frac{f_{m,n+1} - f_{m,n-1}}{2\ \Delta T}\ , \tag{32}$$

$$\frac{\partial^2 f}{\partial T^2}\Big|_{r_m,T_n} = \frac{f_{m,n+1} - 2f_{m,n} + f_{m,n-1}}{\Delta T^2}\ . \tag{33}$$

From equation (31), and secondarily from equations (30), (32), (33), we obtain recursion formulae of the kind

$$f_{m+2,n} = 2f_{m,n} - f_{m-2,n} - (2\ \Delta r)^2 F_{m,n}(c_\nu)\ , \tag{34}$$

see also section 2. The $F_{m,n}$ are very complex, and contain the non-linearities of the Einstein-Maxwell equations. Detailed formulae are available in the Pascal code. (The Pascal code is in the supplementary data.) This method is made possible by the fact that 2nd derivatives in the tensor equations appear always linearly. Therefore the doubling of grid distances in equation (31) was introduced.

When the program runs, the values of the several components are successively quantified in one spherical shell after the other. The computation is done for all components along the inclination (ϑ values) at a given radius, and along the radius (with all inclination values) from outside to inside step by step until geometric limits are reached. After starting the procedure, we get the values as expected from the initial conditions. Suddenly, the values grow over all limits. At this point geometric limits are reached and the calculation is stopped.

The step count (number of iterations) up to the first geometric limit of a metrical component (where the absolute value of the "physical" component becomes unity) depends on the inserted values of the integration constants. A relatively coarse grid reflects strong dependencies, however, the referring values of the integration constants are imprecise. Computations with finer grid lead to smaller contrast of the step counts, but the values are more precise.

The resulting eigenvalues of the integration constants are obtained where the step count until divergence is at maximum. Round-off errors have to be

respected because these can be in the order of step count differences for the formulae.

In order to see the eigenvalues, lots of tests were run with parameters more and less deviating from reference values. The output parameter (used for the plots discussed in the results section) is the mentioned step count. In order to make visible the differences, the step count above a "threshold" is depicted in resulting figures by a more or less fat "point".

Though neutrinos are uncharged, one has to use always the full EINSTEIN-MAXWELL equations (with zero charge and magnetic moments) to account for the inherent non-linearity. Because the information is in the entire field outside the geometric boundary, one has to do so even if charge and magnetic moment are zero. Higher moments exist anyway and are included in the calculation. Only in the (outer) initial conditions (when starting the calculations) they are neglected.

3.3 Computational results

3.3.1 Spins, electric charges, magnetic moments

Tests including parameters different from mass had to be run with an initial radius close to the conjectural particle radius. Here, the influences of the four relevant parameters onto the metric (about 10^{-40}) are comparable.

The best result has been achieved with the free electron, see [7, 10]. The magnetic moment of the electron arises in particularly sharp form, due to the dominant influence. Unfortunately, the mass gets lost in the "noise" from rounding errors. Only cases with charge and mass together can be made visible in exceptional cases, see for example [9].

3.3.2 Masses

The influence of mass on metrics prevails in a certain distance from the conjectural particle or nucleus radius, respectively. It proves being possible to set the remaining parameters to zero.

It was necessary in the pure mass tests to "pile up" the data. For this purpose, several test series with *slightly* different parameters (mostly initial

radius) have been run, and the related step counts (the output) have been added. So the "noise" from rounding errors is successively suppressed. With 80 bit floating point registers, the rounding error is in the 20th decimal. As well, the relative deviation of difference quotients from related differential quotients *in the first step* is roughly 10^{-20} – that is the limit, where the onset of chaotic behaviour can be seen. Consequently, calculations with only 64 bit (double) lead to no meaningful results.

Masses of nuclei

Related tests are reported in [9]. The figures in [9] show up a possible assignment of maxima to nucleus masses in the display. One can see certain patterns in these figures, which could arise from errors by neglecting other parameters.

The tests have been done up to the oxygen nucleus. With appropriate effort, it should be possible to test the whole periodic system of elements, with predictions about its end.

Masses of leptons

It is principally possible to deduce the masses of all free particles, if they are stable to some extent. Since the electron mass is relatively small, one needs an initial radius of about 4×10^{-13} m in order to be able to neglect the influence of spin, charge, magnetic moment to some extent, see Fig. 1 [10]. One step count maximum (piled) appears fairly correctly at the experimental value, flanked by adjoining maxima, possibly caused by the neglected parameters.

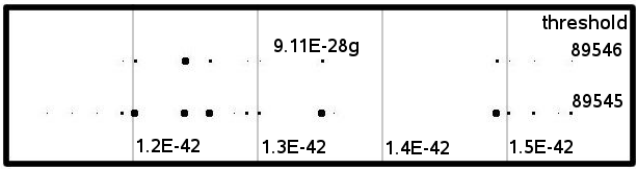

Figure 1: Tests for the free electron. Initial radius 400, 51 values, 9 times piled (459 tests)

The success in detecting known masses gives us confidence for trying a prediction of neutrino masses. That implies that neutrinos are stationary particles, i.e. have rest mass at all. Then they can never reach light speed.

The Particle Data Group [11] commented in the year 2002:
There is now compelling evidence that neutrinos have nonzero mass from the observation of neutrino flavor change, both from the study of atmospheric neutrino fluxes by SuperKamiokande, and from the combined study of solar neutrino cross sections by SNO (charged and neutral currents) and SuperKamiokande (elastic scattering).

The neutrino has the advantage of being electromagnetically neutral. As well, the spin does not perceptibly influence other components of metrics than those for the spin itself. So we can unscrupulously neglect the spin, and search for quite tiny masses.

Quoting the Particle Data Group (in 2002) again [11]:
Mass[4] $m < 3\,\mathrm{eV}$.
Interpretation of tritium beta decay experiments is complicated by anomalies near the endpoint, and the limits are not without ambiguity.
Newer experiments re-verify this ambiguity, just providing multiple mass bounds.

Ten plausible maxima have been found in our calculations for the electron neutrino, see Figs. 2, 3, 4, 5, 6, and the supplementary data. Obtained values are 0.068 eV, 0.095 eV, 0.155 eV, 0.25 eV, 0.31 eV, 0.39 eV, 0.56 eV, 1.63 eV, 2.88 eV, 5.7 eV. Smaller values (Fig. 2) are less convincing.

The mentioned ambiguity goes along with the fact that multiple mass values have been detected. It could be possible that the set of values is reduced by computation with spin. The precision with 80 bit registers is not sufficient for such calculations. However, it could well be possible interpreting some values as composites from smaller values. Here we could have comparable circumstances like in nuclei so that there is no reason for the assumption that only one value can exist. This conclusion is supported by multiple experimental mass bound values.

Many mass values are integer multiples of $\sim 0.08\,\mathrm{eV}$, within the tolerances of the method. At the place of this value there is a hole in the figure, flanked by maxima at 0.068 eV and 0.095 eV. This could be:
1) a methodical error resp. effect, or
2) both values are a kind of basic values, where the other values are composites from.

[4] of electron neutrino

Other interpretations cannot be precluded.

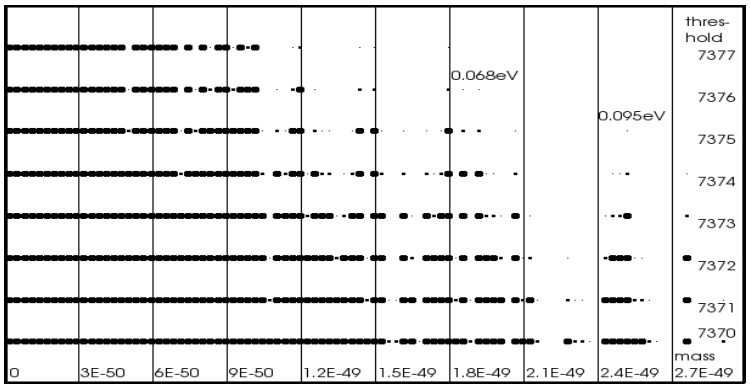

Figure 2: Tests for the electron neutrino, masses $< 0.11\,\mathrm{eV}$. Initial radius 5, 100 values, 9 times piled (900 tests)

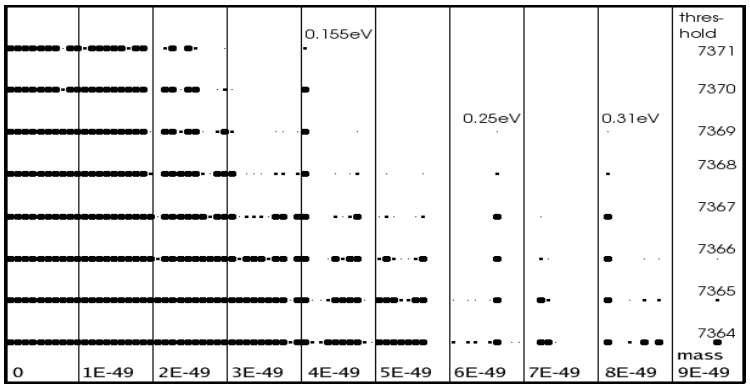

Figure 3: Tests for the electron neutrino, masses $< 0.4\,\mathrm{eV}$. Initial radius 5, 100 values, 9 times piled (900 tests)

4 Conclusion

It has been shown in this paper that neutrino masses can be predicted by numerical calculations based on Einstein-Maxwell theory. Starting from a finite difference scheme for differential equations, chaos properties of these equations were investigated in dependence of parameters being integration constants of the theory. The resulting masses for supposed electron neutrinos

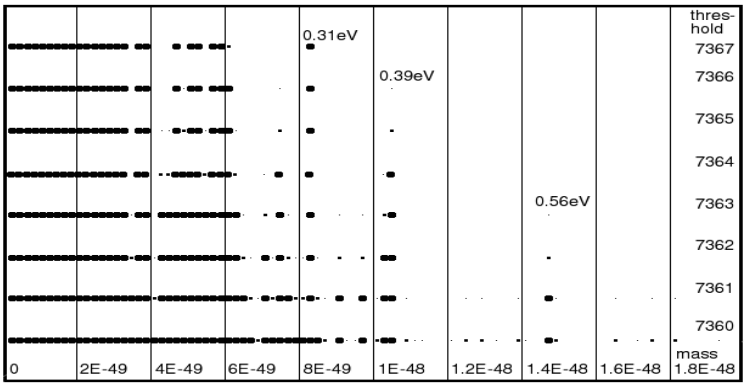

Figure 4: Tests for the electron neutrino, masses $< 1\,\mathrm{eV}$. Initial radius 5, 99 values, 9 times piled (891 tests)

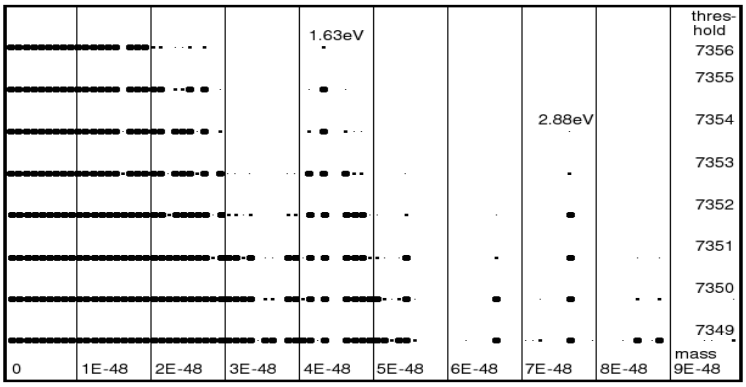

Figure 5: Tests for the electron neutrino, masses $< 4\,\mathrm{eV}$. Initial radius 5, 99 values, 9 times piled (891 tests)

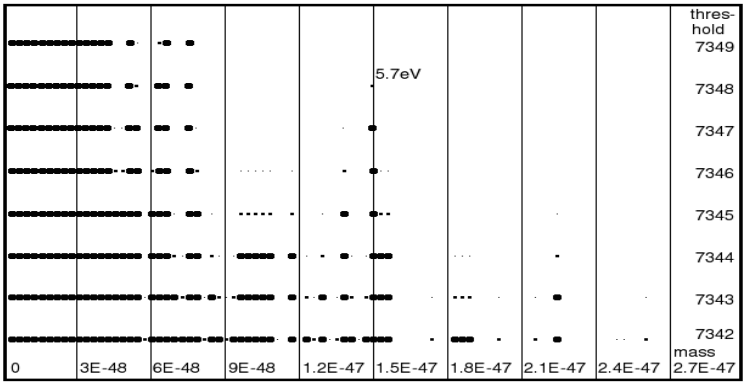

Figure 6: Tests for the electron neutrino, masses $< 11\,\mathrm{eV}$. Initial radius 5, 100 values, 9 times piled (900 tests)

come out to lie in the range being known by experiments. This is probably the first time that supposed neutrino masses are predicted by a theory based on first principles.

ACKNOWLEDGEMENTS. We express our thank to Bernhard Foltz who suggested searching for neutrino masses according to this numerical method. Also, he reported the state of experimental neutrino research.

References

[1] F. W. Hehl, R. A. Puntigam and H. Ruder, (Eds.), *Relativity and Scientific Computing. Computer Algebra, Numerics, Visualization.* Springer-Verlag, Berlin, Heidelberg, 1996.

[2] J. Gleick, *Chaos, die Ordnung des Universums*. Vorstoß in Grenzbereiche der modernen Physik. (Engl. orig.: Chaos. Making a new science. Droemer Knaur München, 1990.

[3] G. Küppers, (Ed.), *Chaos und Ordnung.* Formen der Selbstorganisation in Natur und Gesellschaft. Reclam Ditzingen, 1996.

[4] A. Einstein, *Grundzüge der Relativitätstheorie*. A back-translation from the Four Lectures on Theory of Relativity. Akademie-Verlag Berlin, Pergamon Press Oxford, Friedrich Vieweg & Sohn Braunschweig, 1969.

[5] G.Y. Rainich, Electrodynamics in the General Relativity Theory. *Proc. N.A.S.*, **10**, (1924), 124-127.

[6] G.Y. Rainich, Second Note Electrodynamics in the General Relativity Theory. *Proc. N.A.S.*, **10**, (1924), 294-298.

[7] U.E. Bruchholz, Key Notes on a Geometric Theory of Fields, *Progress in Physics*, **5**(2), (2009), 107-113.
http://www.ptep-online.com/index_files/2009/PP-17-17.PDF

[8] U.E. Bruchholz, Geometry of Space-Time, *Progress in Physics*, **5**(4), (2009), 65-66.
http://www.ptep-online.com/index_files/2009/PP-19-06.PDF

[9] U.E. Bruchholz, Masses of Nuclei Constituted from a Geometric Theory of Fields, *Adv. Studies Theor. Phys.*, **7**(19), (2013), 901-906.
http://dx.doi.org/10.12988/astp.2013.3885

[10] U.E. Bruchholz, How to Deduce Masses and Further Parameters of Particles and Nuclei, *International Journal of Knowledge Based Computer System*, **1**(2), (2013).
http://www.publishingindia.com

[11] K. Hagiwara et al. (Particle Data Group), *Phys. Rev.*, **D 66**, 010001, (2002).
(URL: http://pdg.lbl.gov)